Peroxisomes can oxidize medium- and long-chain fatty acids through a pathway involving ABCD3 and HSD17B4

Sara Violante[1,2,3], Nihad Achetib[1,2], Carlo W. T. van Roermund[4], Jacob Hagen[1,2], Tetyana Dodatko[1,2], Frédéric M. Vaz[4], Hans R. Waterham[4], Hongjie Chen[1,3], Myriam Baes[5], Chunli Yu[1,3], Carmen A. Argmann[1,2], Sander M. Houten[1,2]

[1]Department of Genetics and Genomic Sciences, [2]Icahn Institute for Data Science and Genomic Technology, Icahn School of Medicine at Mount Sinai, 1425 Madison Avenue, Box 1498, New York, NY 10029, USA; [3]Mount Sinai Genomics, Inc, One Gustave L Levy Place #1497 NY, NY 10029; [4]Departments of Clinical Chemistry and Pediatrics, Laboratory Genetic Metabolic Diseases, Academic Medical Center, Amsterdam, The Netherlands; [5]KU Leuven - University of Leuven, Department of Pharmaceutical and Pharmacological Sciences, Laboratory of Cell Metabolism, B-3000 Leuven, Belgium

Running title: Peroxisomal oxidation of mitochondrial fatty acids

Address for correspondence: Sander Houten, Department of Genetics and Genomic Sciences, Icahn School of Medicine at Mount Sinai, 1425 Madison Avenue, Box 1498, New York, NY 10029, USA. Phone: +1 212 659 9222, Fax: +1 212 659 8754, E-mail: sander.houten@mssm.edu

Nonstandard Abbreviations

Cas9, clustered regularly-interspaced short palindromic repeats associated protein 9

CPT, carnitine palmitoyltransferase

CRISPR, clustered regularly-interspaced short palindromic repeats

DCA, dicarboxylic acid

FAO, fatty acid beta-oxidation

L-AC, L-aminocarnitine

KO, knockout

Abstract

Peroxisomes are essential organelles for the specialized oxidation of a wide variety of fatty acids, but they are also able to degrade fatty acids that are typically handled by mitochondria. Using a combination of pharmacological inhibition and CRISPR-Cas9 genome editing technology to simultaneously manipulate peroxisomal and mitochondrial fatty acid oxidation (FAO) in HEK-293 cells, we identified essential players in the metabolic crosstalk between these organelles. Depletion of carnitine palmitoyltransferase 2 (CPT2) activity through pharmacological inhibition or knockout (KO) uncovered a significant residual peroxisomal oxidation of lauric and palmitic acid leading to the production of peroxisomal acylcarnitine intermediates. Generation and analysis of additional single and double KO cell lines revealed that D-bifunctional protein (HSD17B4) and the peroxisomal ABC transporter ABCD3 are essential in peroxisomal oxidation of lauric and palmitic acid. Importantly, our results indicated that peroxisomes not only accept acyl-CoAs, but can also oxidize acylcarnitines in a similar biochemical pathway. By using an *Hsd17b4* KO mouse model, we furthermore demonstrated that peroxisomes contribute to the plasma acylcarnitine profile after acute inhibition of CPT2 proving in vivo relevance of this pathway. We conclude that peroxisomal FAO is important when mitochondrial FAO is defective or overloaded.

Keywords: Fatty acid oxidation; mitochondria; peroxisomes; medium-chain fatty acids; long-chain fatty acids

Introduction

Mitochondrial long-chain fatty acid beta-oxidation (FAO) plays a key role in energy homeostasis as it is a main energy source during fasting (1). Patients with inborn errors of mitochondrial FAO may present with hypoglycemia, and skeletal and cardiac muscle disease illustrating the physiological importance of this pathway in humans (1). Peroxisomes were originally also shown to oxidize long-chain fatty acids such as palmitate akin to mitochondria (2, 3). The identification of peroxisomal disorders, however, led to the characterization of specific substrates for the peroxisomal FAO machinery such as very long-chain fatty acids, long-chain dicarboxylic acids (DCAs), 2-methyl-branched fatty acids and bile acid precursors (4). Although potentially important in patients with a mitochondrial FAO disorder, the metabolic interplay between peroxisomes and mitochondria (5) and a more general role for peroxisomes in the oxidation of long-chain fatty acids have remained largely unexplored.

It is known that peroxisomal FAO contributes to the oxidation of long-chain fatty acids in liver and heart (6-8), but the molecular and biochemical mechanisms and physiological relevance of this pathway are still unknown. In addition, it is well established that under specific conditions such as fasting or in the case of a mitochondrial FAO defect, long-chain fatty acids destined for mitochondria can be omega-oxidized to DCAs by microsomal cytochrome P450 enzymes of the CYP4A family. These long-chain DCAs are then transported to the peroxisome where they are shortened to medium-chain DCAs such as adipic acid. Indeed, the peroxisomal enzyme enoyl-CoA hydratase / 3-hydroxy acyl-CoA dehydrogenase (EHHADH; L-bifunctional protein) is involved in the production of medium-chain DCAs during fasting and dietary intake of medium-chain fatty acids (9, 10). Furthermore, we have recently demonstrated in vitro that in the presence of a defect in mitochondrial FAO, fatty acids can also be redirected to the peroxisomes without prior omega-oxidation (11) (Figure 1A).

Beadle and Tatum demonstrated that genes control specific chemical reactions now known as the one gene-one enzyme hypothesis. Their work was based on the ability to establish mutant *Neurospora* strains by x-ray and the characterization of the resulting vitamin B auxotrophy (12). For many years biochemical genetics research took advantage of similar tools often using the yeast *Saccharomyces cerevisiae*. Forward genetic screens in this model organism have revealed the identity of many genes involved in conserved biochemical pathways, for example the PEX genes in peroxisome biogenesis (13). *S. cerevisiae* was the first eukaryote of which the genome was sequenced, which combined with a relatively simple strategy to disrupt genes, made this yeast ideal for reverse genetics studies. Although RNAi approaches and later zinc finger nucleases and transcription activator-like effector-based nucleases enabled similar studies in human cells, the development of the clustered regularly-interspaced short palindromic repeats (CRISPR)-CRISPR associated protein 9 (Cas9) genome editing technology has significantly advanced the application of biochemical genetics to human cell lines. The main reason for this is that the CRISPR-Cas9 technology allows for the efficient and fast generation of a complete gene knockout (KO) in different cell lines (14).

Additional advantages include the possibility to target multiple genes and generate double or even triple KO cell lines.

Here we used a combination of pharmacological inhibition and CRISPR-Cas9 genome editing technology to identify essential players in the metabolic crosstalk between mitochondria and peroxisomes. We furthermore demonstrated in vivo relevance of this pathway using a mouse model with acute FAO inhibition. Taken together, our findings suggest that there is a tight functional link between mitochondria and peroxisomes, where peroxisomal FAO can serve as a compensatory mechanism in case of mitochondrial FAO defects or mitochondrial overload.

Materials and Methods

Materials

Minimal essential medium (MEM) was obtained from Sigma-Aldrich (St. Louis, MO, USA). Dulbecco's modified Eagle's medium (DMEM), penicillin and streptomycin were obtained from Gibco Invitrogen (Carlsbad, California, USA). Fetal bovine serum was from BioWhittaker Lonza. Lipofectamine 2000 was purchased from Invitrogen (Carlsbad, CA, USA). The CRISPR-Cas9 plasmid (pSpCas9(BB)-2A-GFP; PX458) was obtained via Addgene. HEK-293 cells were obtained from ATCC. The acylcarnitine internal standard mix containing $^{2}H_{9}$-carnitine, $^{2}H_{3}$-acetylcarnitine (C2), $^{2}H_{3}$-propionylcarnitine (C3), $^{2}H_{3}$-butyrylcarnitine (C4), $^{2}H_{9}$-isovalerylcarnitine (C5), $^{2}H_{3}$-octanoylcarnitine (C8), $^{2}H_{9}$-myristoylcarnitine (C14) and $^{2}H_{3}$-palmitoylcarnitine (C16) was from Cambridge Isotope Laboratories (NSK-B, Tewksbury, MA, USA). Bovine serum albumin (BSA, fatty acid free), L-carnitine, lauric acid, palmitic acid, lauroylcarnitine and palmitoylcarnitine were obtained from Sigma-Aldrich (St. Louis, MO, USA). L-aminocarnitine (L-AC; (R)-aminocarnitine, minimum 97%) was obtained from Toronto Research Chemical Inc. (Toronto, ON). (R)-(+)-Etomoxir sodium salt was from Tocris bioscience. All other chemicals were of analytical grade.

Cell culture conditions

HEK-293 cells were cultured in DMEM with 4.5 g/L glucose, 584 mg/L L-glutamine and 25 mM Hepes, supplemented with 10% FBS, 100 U/mL penicillin, 100 mg/mL streptomycin, in a humidified atmosphere of 5% CO_2, at 37ºC.

Generation of CRISPR-Cas9 knockout cell lines

The generation of gene knockout cell lines using the CRISPR-Cas9 genome editing technique was performed essentially as described (14), with minor modifications. For each gene, three different guides were chosen and cloned into the pSpCas9(BB)-2A-GFP vector. Following plasmid purification, HEK-293 cells were transfected using lipofectamin 2000. Forty-eight hours after transfection, the transfected cells with GFP signal were sorted as single cells into 96 well plates by fluorescence activated cell sorting. The clonal cells were cultured for approximately two weeks and subsequently collected for genomic DNA extraction.

We selected 2 independent clonal KO cell lines for *PEX13*, *EHHADH*, *HSD17B4*, *CPT1A*, *CPT2*/*PEX13*, *CPT2*/*ABCD3* and *CPT2*/*CPT1A*. Only 1 clonal KO cell line was obtained for *ABCD3* and *CPT2*. In order to make the mutation analysis simple, we picked clones with homozygous or compound heterozygous nonsense mutations. HEK-293 cells are near triploid with 62–70 chromosomes per cell (15, 16). This implies that cell lines with an apparent homozygous mutation harbored identical triallelic mutations. In apparent compound heterozygous cell lines one of the mutations must be biallelic. Mutation analysis was performed by direct Sanger sequencing of the genomic DNA. Primers (sequences are available

upon request) were chosen to flank the region surrounding the respective guides for each gene (PCR products between 250 and 500 bp). A list of the established cell lines and their mutations is provided in Supplemental table 1. All mutations were predicted to be disease causing - i.e. probably deleterious by MutationTaster (17). In addition, functional assays were performed to validate all the generated KO cell lines except the *EHHADH* KO cell lines. This was due to undetectable protein levels by immunoblotting (GeneTex GTX81126). The *PEX13* KO cell lines were validated using fluorescence microscopy (Figure S1B). The *HSD17B4* and *ABCD3* KO cell lines were validated using immunoblot (Figure S1C, D). The *ABCD3* KO cell lines were validated also by rescuing the phenotype by reintroducing *ABCD3*. The *CPT2* and *CPT2*/*CPT1A* KO cell lines were validated by their aberrant acylcarnitine production. The validations are further detailed below.

Visualization of peroxisomes using fluorescence microscopy

Fluorescence microscopy was performed essentially as described before. Briefly, HEK-293 cell lines were transfected with a plasmid encoding an enhanced green fluorescent protein (GFP)-SKL (18, 19). The SKL is the peroxisomal targeting sequence (i.e. PTS1) that will direct the GFP to the peroxisome enabling its visualization by fluorescence microscopy. *PEX13* KO cells had no detectable peroxisomes (Figure S1B).

Immunoblot analysis

The *HSD17B4* and *ABCD3* KO cell lines were validated by immunoblotting. We used a mouse monoclonal antibody against HSD17B4 at 1:1000 (Abcam ab128565) and a rabbit polyclonal against PMP70 at 1:500 (ABCD3; ThermoFisher, Catalog # PA1-650). The selected *HSD17B4* KO cell lines had undetectable protein levels (Figure S1C). The *ABCD3* single KO and *CPT2*/*ABCD3* double KO cell lines had undetectable ABCD3 protein levels (Figure S1D).

Analysis of fatty acid and acylcarnitine metabolism in HEK-293 cells

The acylcarnitine profiling in HEK-293 cells was performed essentially as described before (11, 20) with minor modifications. HEK-293 cells were seeded in 24 well plates (approximately 100 µg protein per well) and incubated overnight at 37ºC. The following day, the media were removed and 500 µL of the incubation mixture was added to each well. Incubation mixtures contained MEM supplemented with 0.4% BSA (fatty acid free), 0.4 mM L-carnitine and 120 µM lauric acid (C12:0), 120 µM palmitic acid (C16:0), 25 µM lauroylcarnitine (C12-carnitine) or 25 µM palmitoylcarnitine (C16-carnitine). For the inhibition studies, etomoxir and L-AC were added to the incubation mixture at a final concentration of 10 µM and 0-800 µM, respectively. After 72h incubation in a humidified CO_2 incubator (5% CO_2, 95% air) at 37°C, the medium was collected and the cells were washed and resuspended in 100 µL of RIPA buffer to measure protein content using the bicinchoninic acid assay and HSA as standard.

To 20 µL of medium, 100 µL of internal standard mix in methanol was added containing 3.8 µmol/L $^{2}H_{9}$-Carnitine, 0.95 µmol/L $^{2}H_{3}$-C2-carnitine, 0.19 µmol/L $^{2}H_{3}$-C3-carnitine, $^{2}H_{3}$-C4-carnitine, $^{2}H_{9}$-C5-carnitine, $^{2}H_{3}$-C8-carnitine, $^{2}H_{9}$-C14-carnitine and 0.38 µmol/L $^{2}H_{3}$-C16-carnitine. After derivatization of the produced acylcarnitines with 3N 1-butanol/HCl (Regis Technologies), these intermediates were quantified by Electrospray Ionization Tandem Mass Spectrometry (ESI-MS/MS; Agilent 6460 Triple Quad MS) using an established procedure for clinical testing.

Oxidation of [1-^{14}C] C16:0 and [1-^{14}C] C16-carnitine was measured as described before (21).

ABCD3 overexpression

CPT2 KO and *CPT2*/*ABCD3* KO cell lines were transfected with a plasmid containing the human *ABCD3* transporter or the empty vector (pcDNA3) (22). Transfection was performed with Lipofectamine 2000 following the instructions provided by the supplier. After 24h incubation, the cells were loaded with C12:0 or C12-carnitine and the media were analyzed after 72h incubation, as described above.

Animals

All animal experiments were approved either by the IACUC of the Icahn School of Medicine at Mount Sinai and comply with the National Institutes of Health guide for the care and use of Laboratory animals (NIH Publications No. 8023, revised 1978) or by the Research Ethical committee of the KU Leuven (#181/2015). *Ehhadh* KO mice (B6;129P2-*Ehhadh*^{tm1Jkr} (23) were generously provided by Dr. Janardan K. Reddy (Department of Pathology, Feinberg School of Medicine, Northwestern University, Chicago, IL). These mice were crossed with C57BL/6N in order to create a first generation progeny (B6129PF1). The *Ehhadh*$^{+/-}$ mice from the F1 were intercrossed in order to generate an experimental cohort of B6129PF2 mice. From this F2 cohort, male wild type (WT) and *Ehhadh* KO mice were selected. Mice were kept on regular chow and analyzed between 6 and 8 months of age. *Hsd17b4* KO (also called *Mfp2*$^{-/-}$) mice were obtained by intercrossing heterozygous mice on a Swiss/Webster background as previously described (24). All animals received an IP injection of vehicle (0.9% NaCl), L-AC (16 mg/kg) or etomoxir (50 mg/kg) at the end of the afternoon followed by overnight food withdrawal. Mice were euthanized by exsanguination via the vena cava inferior after pentobarbital (100mg/kg IP) anesthesia. Blood was collected for the preparation of EDTA plasma and organs were snap frozen in liquid nitrogen and stored at -80°C for future analyses. Plasma was used for acylcarnitine analysis as described in the previous section. Blood was also collected from the submandibular vein after 8 hours of fasting or in the random fed state with similar results. UPLC-MS/MS analysis of acylcarnitines was performed on pooled plasma from all animals within the groups (25, 26). *Hsd17b4* KO mice and controls received an IP injection of L-AC (16 mg/kg). Blood for plasma isolation was collected from the tail vein after 8 hours of fasting. Two groups of mice were analyzed; one of 4 weeks of age (4 WT and 4 KO) and one of 16-17 weeks of age (4 WT and 4 KO).

Results

Peroxisomal beta-oxidation of lauric acid in HEK-293 cells

HEK-293 cells are easily genetically modified by CRISPR-Cas9 genome editing (14). Here we evaluated whether HEK-293 can be used to measure transfer of mitochondrial substrates to the peroxisome as suggested in our previous work in primary skin fibroblasts (11). To this end, we first generated HEK-293 KO cells for *PEX13*, a crucial gene in peroxisomal biogenesis (27). *PEX13* KO cells had no detectable peroxisomes as demonstrated by the cytosolic localization of GFP-SKL, while control cells showed the typical peroxisomal punctuated fluorescence pattern (Figure S1B).

Long-chain fatty acids such as palmitic acid (C16:0), but also the medium chain fatty acid lauric acid (C12:0) require the action of the carnitine shuttle before they can be oxidized in the mitochondrial matrix (28) (Figure 1A). We have shown that upon inhibition of carnitine palmitoyltransferase 2 (CPT2) with L-aminocarnitine (L-AC), fatty acids can be rerouted to the peroxisome for alternative FAO resulting in the production of medium- and short-chain acylcarnitines that will accumulate in the extracellular media (11). L-AC reveals the production of peroxisomal acylcarnitines not only due to its general inhibition of mitochondrial FAO (29), but also because it prevents peroxisomal acylcarnitines from entering the mitochondria for full oxidation (11). In order to measure peroxisomal acylcarnitine production, control and *PEX13* KO HEK-293 cells were incubated with C12:0 and increasing concentrations of L-AC. Media of control HEK-293 cells incubated with L-AC and C12:0 showed accumulation of C12-, C10-, C8- and C6-carnitine. Media of the *PEX13* KO cells failed to accumulate C10-, C8- and C6-carnitine proving their peroxisomal origin (Figure 1B, S1E). Thus HEK-293 cells are capable of oxidizing C12:0 in the peroxisome. For the remainder of the paper, we focus on C10-carnitine as the main marker for peroxisomal fatty acid oxidation.

HSD17B4 and ABCD3 are essential for oxidation of lauric acid

Peroxisomal FAO follows a mechanism that involves dehydrogenation, hydration, a second dehydrogenation and thiolytic cleavage, similar to mitochondrial FAO (4). The second and third step are catalyzed by the D- and L-bifunctional protein encoded by *HSD17B4* and *EHHADH*, respectively (Figure 1A). Both genes are expressed in HEK-293 cells, although *EHHADH* at a relatively low level (Figure S1A). We used CRISPR-Cas9 genome editing to generate KO cell lines for both genes. Next, we loaded the cells with C12:0 and inhibited the carnitine shuttle with L-AC in order to monitor the peroxisomal acylcarnitine production. While *EHHADH* KO cells produced levels of C10-carnitine similar to controls, this metabolite was severely reduced in *HSD17B4* KO cells (Figure 1B). This indicates that *HSD17B4* is important for the peroxisomal oxidation of medium-chain fatty acids, while *EHHADH* is either not involved or not essential in HEK-293 cells.

Next, we focused on the peroxisomal import of fatty acids. This process is mediated by three ATP-binding cassette transporters, ABCD1, 2 and 3. Based on the reported expression levels of these ABC transporters in HEK-293 cells (Figure S1A) and the established substrate specificities (30), we speculated that ABCD3 would transport C12:0 to the peroxisome. Therefore, we targeted this gene using CRISPR-Cas9 genome editing generating *ABCD3* KO cell lines. Upon loading with C12:0 and L-AC, *ABCD3* KO cells failed to accumulate C10-carnitine (Figure 1B) suggesting that transport mediated by ABCD3 is crucial in the peroxisomal degradation of medium-chain fatty acids.

CPT2 KO cells further implicate ABCD3 in peroxisomal lauric acid metabolism

In order to avoid potential problems of the pharmacological inhibition of mitochondrial FAO using L-AC, we next generated *CPT2* KO cell lines using CRISPR-Cas9 genome editing in control HEK-293 and the existing *PEX13* and *ABCD3* KO cell lines. Incubation of CPT2 KO cells with C12:0 led to a more pronounced accumulation of C10-carnitine when compared to the condition in which CPT2 was inhibited by L-AC (Figures 1B and 2A). This difference may be due to a lack of specificity of L-AC for CPT2 at higher concentrations or the competitive nature of the inhibition (29). We note again that there is also peroxisomal production of C8- and C6-carnitine (Figure S1F). The production of C10-carnitine is absent in *CPT2*/*PEX13* and *CPT2*/*ABCD3* double KO cells confirming that ABCD3 is involved in the peroxisomal generation of this intermediate (Figure 2A).

To further establish the role of ABCD3 in this pathway, we overexpressed *ABCD3* in the *CPT2* KO and *CPT2*/*ABCD3* KO cell lines and loaded these cells with C12:0. Overexpression of *ABCD3* restored the production of C10-carnitine in *CPT2*/*ABCD3* KO cells (Figure 2B). These data unequivocally establish that ABCD3 is required for transport of medium-chain fatty acids across the peroxisomal membrane.

Peroxisomal beta-oxidation of palmitic acid in HEK-293 cells

We next investigated peroxisomal metabolism of C16:0, which is a common fatty acid in most diets. Upon loading with C16:0 we were unable to detect C10- and C12-carnitine after inhibition of CPT2 with L-AC, but these metabolites were detectable in *CPT2* KO cells. The levels of C10- and C12-carnitine were lower in media of *CPT2*/*PEX13* and *CPT2*/*ABCD3* KO cells when compared to *CPT2* KO cells evidencing their peroxisomal origin (Figure 3A, S1G). These data indicate that C16:0 can also be metabolized in peroxisomes when mitochondrial FAO is defective.

To provide additional evidence for the peroxisomal oxidation of long-chain fatty acids, we measured production of CO_2 and acid soluble products from [1-^{14}C] C16:0. C16:0 oxidation in *CPT2* KO cells was 13% of control HEK-293 cells, but clearly detectable (Figure 3B). C16:0 oxidation decreased to 1% in *CPT2*/*PEX13* and *CPT2*/*ABCD3* KO (Figure 3B). This further proves that peroxisomes can contribute significantly to long-chain FAO.

Peroxisomes can accept acylcarnitines as substrate

After identifying some of the molecular players in this pathway, we aimed to further characterize the mechanism by which these fatty acids are transported into the peroxisome. The peroxisomal ABC transporters are thought to transport acyl-CoA intermediates. The acyl-CoA is hydrolyzed by intrinsic thioesterase activity of the transporter during transit leaving a free fatty acid in the peroxisome (31). Our previous work using a combination of CPT1 and CPT2 inhibitors suggested that C12:0 has better access to the peroxisome as C12-carnitine than as the acyl-CoA derivative (11). Consistently, we now show that C12- and C16-carnitine can undergo peroxisomal FAO when CPT2 is blocked in a process that depends on ABCD3 (Figure 4A). To further investigate whether peroxisomes can accept acylcarnitines as substrate, we inhibited CPT1 using the irreversible inhibitor etomoxir preventing the reconversion of the acylcarnitine into the respective CoA ester (Figure 1A). The CPT2 KO cell lines incubated with etomoxir and C12-carnitine still showed production of peroxisomal C10-carnitine (Figure 4B), which suggests that C12-carnitine has direct access to the peroxisome.

To overcome potential unintended effects of pharmacologic inhibition using etomoxir, we removed the activity of both acyltransferases by generating *CPT2*/*CPT1A* double KO cell lines. The successful targeting of *CPT1A* is confirmed by a pronounced defect in C16-carnitine production after incubation of the double KO cells with C16:0 (Figure 4C). We incubated *CPT2* KO and *CPT2*/*CPT1A* KO cells with C12:0, C12-carnitine, C16:0 or C16-carnitine (Figure 4D for C12 and Figure 4E for C16). The production of the peroxisomal C10-carnitine from all these substrates was not affected by the additional loss of CPT1A (Figure 4D and E). This strongly suggests that C12 and C16 not only have direct access to the peroxisome as acyl-CoAs, but also as acylcarnitines. The accumulation of C10-carnitine after incubation with C12-carnitine is 50% in comparison with C12:0 incubation indicating that the transport of C12-carnitine esters may be less efficient than that of C12-CoA, or that the peroxisomal conversion of acylcarnitines into the respective acyl-CoAs (likely via carnitine octanoyltransferase) may be a rate limiting step (Figure 4D).

Overall our data suggest that peroxisomes accept the CoA and carnitine ester of C12:0 and C16:0 as substrate in a mechanism possibly involving ABCD3. We next measured production of CO_2 and acid soluble products from [1-^{14}C] C16-carnitine. Oxidation of C16-carnitine was not impaired in *CPT1A* KO HEK-293 cells, which illustrates that extracellular C16-carnitine is effectively used for mitochondrial oxidation and its (enzymatic) hydrolysis is negligible. Oxidation of C16-carnitine in *CPT2* and *CPT2*/*CPT1A* KO was detectable, but only 2% of control HEK-293 cells. Oxidation of C16-carnitine in *CPT2*/*PEX13* and *CPT2*/*ABCD3* was virtually undetectable (Figure 4F). Overall our results indicate that peroxisomes have the ability to accept acylcarnitines as substrates.

Peroxisomal acylcarnitines are detectable in plasma of mice after pharmacological inhibition of FAO

Multiple case reports of CPT2-deficient patients describe that in addition to the prominent increase in plasma C16- and C18:1-carnitine there are also elevations of C12- and C14-acylcarnitines (32-37). Our

work suggests that these metabolites have a peroxisomal origin. In order to study peroxisomal FAO of long-chain fatty acids in a mitochondrial FAO defect in vivo, we administered L-AC and etomoxir to WT mice followed by overnight food withdrawal. As expected, the CPT2 inhibition resulted in pronounced accumulation of long-chain acylcarnitine species in the plasma of these animals, specifically C16-, C18:1- and C18-carnitine. Treated animals also present a significantly higher ratio (C16+C18:1)/C2, which is commonly used for the clinical diagnosis of CPT2 deficiency (Figure 5A). We also observed an increased concentration of several other acylcarnitines in the treated animals including C10:1-, C10-, C12:1-, C12-, C14:1- and C14-carnitine (Figure 5B). Additional quantification of the C14:1-carnitines using UPLC-MS/MS analysis demonstrated that the majority was cis-5-tetradecenoylcarnitine (Figure 5C). In contrast to cis-9-tetradecenoate (myristoleic acid), cis-5-tetradecenoate is not a dietary fatty acid, but derived from oleate oxidation (38). Mitochondrial FAO inhibition with etomoxir, did not lead to a significant accumulation of any acylcarnitine species (Figure 5A, B). Analysis of liver acylcarnitines yielded results similar to plasma (not shown). We conclude that given the inhibition of mitochondrial FAO at the level of CPT2, the in vivo accumulation of these non-dietary C10-, C12- and C14-acylcarnitines in plasma is likely mediated by peroxisomal oxidation.

Similar to our in vitro experiments, we next investigated whether D- (HSD17B4) or L-bifunctional (EHHAHD) protein is involved in the production of peroxisomal acylcarnitines in vivo upon CPT2 inhibition. For this, we administered L-AC to *Hsd17b4* KO, *Ehhadh* KO and WT mice. The concentrations of C10-, C12:1-, C12-, C14- and C16:1-carnitine were significantly lower in *Hsd17b4* KO mice when compared to the controls. The concentrations of C16-, C18:2-, C18:1- and C18-carnitine were not different between *Hsd17b4* KO and WT mice (Figure 5D, E). The results in the *Ehhadh* KO mice were not different when compared to their WT counterparts (Figure 5A, B). Taken together, these animal studies indicate that CPT2 inhibition leads to the production of peroxisomal acylcarnitines. HSD17B4 appears to be the major peroxisomal bifunctional enzyme involved in the generation of these intermediates.

Discussion

The potential role of peroxisomal FAO as an alternative pathway when mitochondrial FAO is impaired or overloaded has remained largely unexplored. We have previously shown that when mitochondrial FAO is defective in fibroblasts, peroxisomes can take up and oxidize C12:0, a fatty acid that is normally metabolized within the mitochondria (11). In order to define the molecular players of this process, we used CRISPR-Cas9 genome editing to perform a classic reverse genetics study in which we disrupted genes of interest in mitochondrial or peroxisomal FAO and observed the biochemical phenotype by measuring the production of the peroxisomal acylcarnitines such as C10-carnitine. We aimed to identify the enzymes and transporters involved in the peroxisomal FAO of medium- and long-chain fatty acids when mitochondrial FAO is defective. We started by investigating the role of L- and D-bifunctional proteins (encoded by *EHHADH* and *HDS17B4*, respectively) that catalyze the second and third step in peroxisomal FAO. EHHADH was an attractive candidate gene because it is highly inducible and has an established role in the oxidation of long- and medium-chain DCAs (9, 10). However, upon inhibition of mitochondrial FAO and loading with C12:0, *EHHADH* KO cell lines produced C10-carnitine levels similar to control cell lines. This suggests that this enzyme is not involved, or at least it is not essential in the peroxisomal degradation of medium-chain fatty acids in HEK-293 cells. In contrast, *HSD17B4* KO cells incubated with C12:0 showed a marked decrease in the production of C10-carnitine, which indicates that this enzyme is involved in the peroxisomal FAO of C12:0. In contrast to *PEX13* KO cell lines, the *HSD17B4* KO did produce small amounts of C10-carnitine (Figure 1B). Given the predicted severity of the *HSD17B4* mutations and the resulting absence of the protein, it is unlikely that this is due to residual HSD17B4 activity. Therefore, we speculate that despite its low expression in HEK-293 cells, EHHADH can partially compensate for the loss of HSD17B4. We obtained similar results in animal studies in which we administered L-AC to WT, *Ehhadh* KO and *Hsd17b4* KO mice. The concentration of C10-, C12:1- and C12-carnitine increased upon L-AC administration. We observed no differences in the plasma concentration of these acylcarnitines between WT and *Ehhadh* KO animals. These metabolites were significantly lower in *Hsd17b4* KO mice, but not absent. This proves their peroxisomal origin, but also indicates that HSD17B4 is not the only source with EHHADH being the most likely alternative source. The identity of the enzymes that catalyze the first and last step in peroxisomal FAO will be addressed in future studies.

We also studied the mechanism by which mitochondrial FAO substrates cross the peroxisomal membrane. The peroxisomal transporter ABCD3 is well expressed in HEK-293 cells and known to transport a variety of fatty acids including C16:0 (30). *ABCD3* KO cell lines failed to produce C10-carnitine from both C12:0 and C16:0. This proves that ABCD3 is crucial in the transport of mitochondrial substrates into peroxisomes in HEK-293 cells. ABCD1 and ABCD2 have been demonstrated to transport C16:0 as well (30). ABCD1 is lowly expressed in HEK-293 cells, whereas expression of ABCD2 expression is absent, which likely explains their negligible contribution to the peroxisomal oxidation of C16:0 and C12:0 in the

HEK-293 cell system. This expression profile of the peroxisomal ABC transporters in HEK-293 cells mirrors the expression profile in major fatty acid catabolizing organs such as liver and kidney (39). We therefore argue that ABCD3 likely plays a major role in the transport of mitochondrial substrates into peroxisomes in physiologically relevant tissues. We, however, cannot exclude that ABCD1 and ABCD2 can contribute to this process in tissues with significant expression of these transporters.

We have shown here that specific metabolites accumulating in mitochondrial FAO defects can be directed to the peroxisome for alternative FAO. The peroxisomal ABC transporters are known to accept acyl-CoAs as substrate. There are currently two models for acyl-CoA transport, one where acyl-CoAs enter the peroxisome directly (40), and another where the acyl-CoA is hydrolyzed during transport and re-esterified in the peroxisomal matrix (31). The ABC transporters contain intrinsic thioesterase activity that allows the cleavage of the CoA moiety (41). This second model of transport is currently favored. Our data suggest that acylcarnitines might be an alternative substrate for ABCD3. To investigate this we used the *CPT2* KO cell model and disrupted CPT1A activity either pharmacologically or by using CRISPR-Cas9. The impairment of CPT1A will prevent the conversion of acyl-CoAs into acylcarnitines, but also the reverse activity in which the acylcarnitine is converted into an acyl-CoA. We show that in the *CPT2*/*CPT1A* double KO cell lines, C12- and C16-carnitine are oxidized in the peroxisome, which is evidenced by the production of peroxisomal acylcarnitines and a low but detectable oxidation of [1-^{14}C] C16-carnitine. This indicates that in addition to acyl-CoAs, acylcarnitines are a possible substrate for peroxisomes. This finding may not be completely unexpected given the strong evidence that peroxisomes are able to produce acylcarnitines (42-48). One potential pitfall of our experiment may be the presence of carboxylesterases. These enzymes can catalyze the hydrolysis of many endogenous compounds including acylcarnitines (49, 50). Thus in a *CPT2*/*CPT1A* double KO cell line, a carboxylesterase may hydrolyze the acylcarnitine and the resulting fatty acid could then be reactivated to an acyl-CoA. Carboxylesterases, however, are mainly localized in the endoplasmic reticulum and such a mechanism seems therefore unlikely. Indeed, our results show that extracellular C16-carnitine is an effective substrate for mitochondrial FAO and thus hydrolysis of the carnitine ester appears negligible. Definite proof that acylcarnitines can be directly transported into peroxisomes by ABCD3 or other transporters will require reconstitution of these proteins in liposomes and subsequent transport studies. Unfortunately, such studies have proven challenging and have not been reported yet.

It has been speculated that acylcarnitines would cross the peroxisomal membrane through unspecific membrane channels (such as PXMP2), which are permeable to compounds up to 400 Da (51). We show that medium- and long-chain acylcarnitines depend on the ABCD3 transporter to reach the peroxisomal matrix for FAO arguing against a model in which these metabolites simply diffuse into the peroxisome.

The incubation of *CPT2* KO cells with C16:0 led to the production of peroxisomal C10- and C12-carnitine intermediates illustrating that peroxisomes can handle these abundant dietary fatty acids. Importantly, analysis of plasma acylcarnitine profiles in patients diagnosed with CPT2 deficiency has also

revealed an accumulation of medium-chain acylcarnitines (32-37). Using L-AC in mice, we were able to reproduce a similar acylcarnitine profile with a pronounced increase in C10-, C12- and C14- saturated and unsaturated species. Fatty acids with these chain-lengths are not part of a regular mouse chow or human diet. Therefore similar to the cell-based experiments, these acylcarnitines must be derived from peroxisomal degradation of the long-chain fatty acids. Indeed, the concentrations of C10-, C12:1- and C12-carnitine were lower in *Hsd17b4* KO mice after administration of L-AC. These results establish that peroxisomal FAO can be an alternative in vivo pathway when mitochondrial FAO is defective. Of note, inhibition of mitochondrial FAO using etomoxir in mice did not lead to a detectable production of peroxisomal acylcarnitine species. We speculate that in etomoxir-treated animals, the accumulating long-chain acyl-CoA esters will be partially oxidized in the peroxisome. However, as the mitochondrial CPT2 is functional, the resulting peroxisomal medium-chain acylcarnitines can be transferred to the mitochondria and fully oxidized explaining their absence in the plasma acylcarnitine profile.

In summary, we have demonstrated, in vitro and in vivo, that peroxisomes accept and oxidize medium- and long-chain fatty acids in a pathway that involves HSD17B4 and ABCD3. Our work suggests that peroxisomal FAO is a relevant pathway for alternative metabolism in mitochondrial long-chain FAO deficiencies such as CPT2, very long-chain acyl-CoA dehydrogenase (VLCAD) and long-chain hydroxyacyl-CoA dehydrogenase (LCHAD) deficiency. Future studies should consider this pathway in the pathophysiology and treatment of long-chain FAO deficiencies.

Acknowledgments

We would like to thank Janet Koster (Academic Medical Center, Amsterdam) for providing the ABCD3 plasmid, Ethellyn Panta and Tara Singh (Clinical Biochemical Genetics, Icahn School of Medicine at Mount Sinai, New York) for the assistance with the acylcarnitine measurements, and Benny Das (University of Leuven, Belgium) for technical assistance.

Research reported in this publication was supported by the National Institute of Diabetes and Digestive and Kidney Diseases of the National Institutes of Health under Award Number 5R01DK113172-02. The content is solely the responsibility of the authors and does not necessarily represent the official views of the National Institutes of Health.

Author Contributions

Sara Violante, Carmen Argmann and Sander Houten designed research. Sara Violante, Nihad Achetib, Carlo van Roermund, Jacob Hagen, Tetyana Dodatko performed the research. Myriam Baes, Frédéric Vaz, Hans Waterham, Hongjie Chen and Chunli Yu contributed new reagents or analytic tools. Sara Violante and Sander Houten analyzed data. Sara Violante and Sander Houten wrote the paper.

References

1. Houten, S. M., Violante, S., Ventura, F. V., and Wanders, R. J. (2016) The biochemistry and physiology of mitochondrial fatty acid beta-oxidation and its genetic disorders. *Annu Rev Physiol* **78**, 23-44
2. Lazarow, P. B. (1978) Rat liver peroxisomes catalyze the beta oxidation of fatty acids. *J Biol Chem* **253**, 1522-1528
3. Lazarow, P. B. (1977) Three hypolipidemic drugs increase hepatic palmitoyl-coenzyme A oxidation in the rat. *Science* **197**, 580-581
4. Wanders, R. J., and Waterham, H. R. (2006) Biochemistry of mammalian peroxisomes revisited. *Annu. Rev. Biochem.* **75**, 295-332
5. Schrader, M., Costello, J., Godinho, L. F., and Islinger, M. (2015) Peroxisome-mitochondria interplay and disease. *Journal of inherited metabolic disease* **38**, 681-702
6. Reszko, A. E., Kasumov, T., David, F., Jobbins, K. A., Thomas, K. R., Hoppel, C. L., Brunengraber, H., and Des Rosiers, C. (2004) Peroxisomal fatty acid oxidation is a substantial source of the acetyl moiety of malonyl-CoA in rat heart. *J Biol Chem* **279**, 19574-19579
7. Bian, F., Kasumov, T., Thomas, K. R., Jobbins, K. A., David, F., Minkler, P. E., Hoppel, C. L., and Brunengraber, H. (2005) Peroxisomal and mitochondrial oxidation of fatty acids in the heart, assessed from the 13C labeling of malonyl-CoA and the acetyl moiety of citrate. *J Biol Chem* **280**, 9265-9271
8. Kasumov, T., Adams, J. E., Bian, F., David, F., Thomas, K. R., Jobbins, K. A., Minkler, P. E., Hoppel, C. L., and Brunengraber, H. (2005) Probing peroxisomal beta-oxidation and the labelling of acetyl-CoA proxies with [1-(13C)]octanoate and [3-(13C)]octanoate in the perfused rat liver. *Biochem J* **389**, 397-401
9. Houten, S. M., Denis, S., Argmann, C. A., Jia, Y., Ferdinandusse, S., Reddy, J. K., and Wanders, R. J. (2012) Peroxisomal L-bifunctional enzyme (Ehhadh) is essential for the production of medium-chain dicarboxylic acids. *Journal of lipid research* **53**, 1296-1303
10. Ding, J., Loizides-Mangold, U., Rando, G., Zoete, V., Michielin, O., Reddy, J. K., Wahli, W., Riezman, H., and Thorens, B. (2013) The peroxisomal enzyme L-PBE is required to prevent the dietary toxicity of medium-chain fatty acids. *Cell reports* **5**, 248-258
11. Violante, S., IJlst, L., te Brinke, H., Koster, J., Tavares de Almeida, I., Wanders, R. J., Ventura, F. V., and Houten, S. M. (2013) Peroxisomes contribute to the acylcarnitine production when the carnitine shuttle is deficient. *Biochim Biophys Acta* **1831**, 1467-1474
12. Beadle, G. W., and Tatum, E. L. (1941) Genetic Control of Biochemical Reactions in Neurospora. *Proc Natl Acad Sci U S A* **27**, 499-506
13. Subramani, S. (1993) Protein import into peroxisomes and biogenesis of the organelle. *Annu Rev Cell Biol* **9**, 445-478
14. Ran, F. A., Hsu, P. D., Wright, J., Agarwala, V., Scott, D. A., and Zhang, F. (2013) Genome engineering using the CRISPR-Cas9 system. *Nature protocols* **8**, 2281-2308
15. Bylund, L., Kytola, S., Lui, W. O., Larsson, C., and Weber, G. (2004) Analysis of the cytogenetic stability of the human embryonal kidney cell line 293 by cytogenetic and STR profiling approaches. *Cytogenetic and genome research* **106**, 28-32
16. Lin, Y. C., Boone, M., Meuris, L., Lemmens, I., Van Roy, N., Soete, A., Reumers, J., Moisse, M., Plaisance, S., Drmanac, R., Chen, J., Speleman, F., Lambrechts, D., Van de Peer, Y., Tavernier, J., and Callewaert, N. (2014) Genome dynamics of the human embryonic kidney 293 lineage in response to cell biology manipulations. *Nature communications* **5**, 4767
17. Schwarz, J. M., Cooper, D. N., Schuelke, M., and Seelow, D. (2014) MutationTaster2: mutation prediction for the deep-sequencing age. *Nature methods* **11**, 361-362
18. Waterham, H. R., Koster, J., van Roermund, C. W., Mooyer, P. A., Wanders, R. J., and Leonard, J. V. (2007) A lethal defect of mitochondrial and peroxisomal fission. *N.Engl.J.Med.* **356**, 1736-1741
19. Ebberink, M. S., Mooijer, P. A., Gootjes, J., Koster, J., Wanders, R. J., and Waterham, H. R. (2011) Genetic classification and mutational spectrum of more than 600 patients with a Zellweger syndrome spectrum disorder. *Hum.Mutat.* **32**, 59-69
20. Ventura, F. V., Costa, C. G., Struys, E. A., Ruiter, J., Allers, P., IJlst, L., de Almeida, I. T., Duran, M., Jakobs, C., and Wanders, R. J. (1999) Quantitative acylcarnitine profiling in fibroblasts using

[U-13C] palmitic acid: an improved tool for the diagnosis of fatty acid oxidation defects. *Clin. Chim. Acta* **281**, 1-17
21. Wanders, R. J., Denis, S., Ruiter, J. P., Schutgens, R. B., van Roermund, C. W., and Jacobs, B. S. (1995) Measurement of peroxisomal fatty acid beta-oxidation in cultured human skin fibroblasts. *Journal of inherited metabolic disease* **18 Suppl 1**, 113-124
22. Ferdinandusse, S., Jimenez-Sanchez, G., Koster, J., Denis, S., Van Roermund, C. W., Silva-Zolezzi, I., Moser, A. B., Visser, W. F., Gulluoglu, M., Durmaz, O., Demirkol, M., Waterham, H. R., Gokcay, G., Wanders, R. J., and Valle, D. (2015) A novel bile acid biosynthesis defect due to a deficiency of peroxisomal ABCD3. *Hum Mol Genet* **24**, 361-370
23. Qi, C., Zhu, Y., Pan, J., Usuda, N., Maeda, N., Yeldandi, A. V., Rao, M. S., Hashimoto, T., and Reddy, J. K. (1999) Absence of spontaneous peroxisome proliferation in enoyl-CoA Hydratase/L-3-hydroxyacyl-CoA dehydrogenase-deficient mouse liver. Further support for the role of fatty acyl CoA oxidase in PPARalpha ligand metabolism. *J. Biol. Chem.* **274**, 15775-15780
24. Baes, M., Huyghe, S., Carmeliet, P., Declercq, P. E., Collen, D., Mannaerts, G. P., and Van Veldhoven, P. P. (2000) Inactivation of the peroxisomal multifunctional protein-2 in mice impedes the degradation of not only 2-methyl-branched fatty acids and bile acid intermediates but also of very long chain fatty acids. *J.Biol.Chem.* **275**, 16329-16336
25. Minkler, P. E., Stoll, M. S., Ingalls, S. T., Kerner, J., and Hoppel, C. L. (2015) Validated method for the quantification of free and total carnitine, butyrobetaine, and acylcarnitines in biological samples. *Analytical chemistry* **87**, 8994-9001
26. Minkler, P. E., Stoll, M. S., Ingalls, S. T., Kerner, J., and Hoppel, C. L. (2015) Quantitative acylcarnitine determination by UHPLC-MS/MS--Going beyond tandem MS acylcarnitine "profiles". *Mol Genet Metab* **116**, 231-241
27. Waterham, H. R., and Ebberink, M. S. (2012) Genetics and molecular basis of human peroxisome biogenesis disorders. *Biochim.Biophys.Acta* **1822**, 1430-1441
28. Violante, S., IJlst, L., te Brinke, H., Tavares de Almeida, I., Wanders, R. J., Ventura, F. V., and Houten, S. M. (2013) Carnitine palmitoyltransferase 2 and carnitine/acylcarnitine translocase are involved in the mitochondrial synthesis and export of acylcarnitines. *FASEB J.* **27**, 2039-2044
29. Chegary, M., te Brinke, H., Doolaard, M., IJlst, L., Wijburg, F. A., Wanders, R. J., and Houten, S. M. (2008) Characterization of L-aminocarnitine, an inhibitor of fatty acid oxidation. *Mol. Genet. Metab.* **93**, 403-410
30. van Roermund, C. W., IJlst, L., Wagemans, T., Wanders, R. J., and Waterham, H. R. (2014) A role for the human peroxisomal half-transporter ABCD3 in the oxidation of dicarboxylic acids. *Biochim Biophys Acta* **1841**, 563-568
31. Baker, A., Carrier, D. J., Schaedler, T., Waterham, H. R., van Roermund, C. W., and Theodoulou, F. L. (2015) Peroxisomal ABC transporters: functions and mechanism. *Biochem Soc Trans* **43**, 959-965
32. Hurvitz, H., Klar, A., Korn-Lubetzki, I., Wanders, R. J., and Elpeleg, O. N. (2000) Muscular carnitine palmitoyltransferase II deficiency in infancy. *Pediatr Neurol* **22**, 148-150
33. Fontaine, M., Briand, G., Largilliere, C., Degand, P., Divry, P., Vianey-Saban, C., Mousson, B., and Vamecq, J. (1998) Metabolic studies in a patient with severe carnitine palmitoyltransferase type II deficiency. *Clinica chimica acta; international journal of clinical chemistry* **273**, 161-170
34. Anichini, A., Fanin, M., Vianey-Saban, C., Cassandrini, D., Fiorillo, C., Bruno, C., and Angelini, C. (2011) Genotype-phenotype correlations in a large series of patients with muscle type CPT II deficiency. *Neurological research* **33**, 24-32
35. Yamada, K., Bo, R., Kobayashi, H., Hasegawa, Y., Ago, M., Fukuda, S., Yamaguchi, S., and Taketani, T. (2017) A newborn case with carnitine palmitoyltransferase II deficiency initially judged as unaffected by acylcarnitine analysis soon after birth. *Mol Genet Metab Rep* **11**, 59-61
36. Wieser, T. (2004) Carnitine Palmitoyltransferase II Deficiency. In *GeneReviews® [Internet]* (Adam, M. P., Ardinger, H. H., Pagon, R. A., and Wallace, S. E., eds), University of Washington, Seattle, Seattle (WA)
37. Albers, S., Marsden, D., Quackenbush, E., Stark, A. R., Levy, H. L., and Irons, M. (2001) Detection of neonatal carnitine palmitoyltransferase II deficiency by expanded newborn screening with tandem mass spectrometry. *Pediatrics* **107**, E103

38. Chegary, M., te Brinke, H., Ruiter, J. P., Wijburg, F. A., Stoll, M. S., Minkler, P. E., van Weeghel, M., Schulz, H., Hoppel, C. L., Wanders, R. J., and Houten, S. M. (2009) Mitochondrial long chain fatty acid beta-oxidation in man and mouse. *Biochim. Biophys. Acta* **1791**, 806-815
39. GTEx-Consortium. (2015) Human genomics. The Genotype-Tissue Expression (GTEx) pilot analysis: multitissue gene regulation in humans. *Science* **348**, 648-660
40. Wiesinger, C., Kunze, M., Regelsberger, G., Forss-Petter, S., and Berger, J. (2013) Impaired very long-chain acyl-CoA beta-oxidation in human X-linked adrenoleukodystrophy fibroblasts is a direct consequence of ABCD1 transporter dysfunction. *J Biol Chem* **288**, 19269-19279
41. De Marcos Lousa, C., van Roermund, C. W., Postis, V. L., Dietrich, D., Kerr, I. D., Wanders, R. J., Baldwin, S. A., Baker, A., and Theodoulou, F. L. (2013) Intrinsic acyl-CoA thioesterase activity of a peroxisomal ATP binding cassette transporter is required for transport and metabolism of fatty acids. *Proc Natl Acad Sci U S A* **110**, 1279-1284
42. Verhoeven, N. M., Roe, D. S., Kok, R. M., Wanders, R. J., Jakobs, C., and Roe, C. R. (1998) Phytanic acid and pristanic acid are oxidized by sequential peroxisomal and mitochondrial reactions in cultured fibroblasts. *J Lipid Res* **39**, 66-74
43. Choi, S. J., Oh, D. H., Song, C. S., Roy, A. K., and Chatterjee, B. (1995) Molecular cloning and sequence analysis of the rat liver carnitine octanoyltransferase cDNA, its natural gene and the gene promoter. *Biochim Biophys Acta* **1264**, 215-222
44. Miyazawa, S., Ozasa, H., Osumi, T., and Hashimoto, T. (1983) Purification and properties of carnitine octanoyltransferase and carnitine palmitoyltransferase from rat liver. *J Biochem* **94**, 529-542
45. Farrell, S. O., Fiol, C. J., Reddy, J. K., and Bieber, L. L. (1984) Properties of purified carnitine acyltransferases of mouse liver peroxisomes. *J Biol Chem* **259**, 13089-13095
46. Farrell, S. O., and Bieber, L. L. (1983) Carnitine octanoyltransferase of mouse liver peroxisomes: properties and effect of hypolipidemic drugs. *Arch Biochem Biophys* **222**, 123-132
47. Jakobs, B. S., and Wanders, R. J. (1995) Fatty acid beta-oxidation in peroxisomes and mitochondria: the first, unequivocal evidence for the involvement of carnitine in shuttling propionyl-CoA from peroxisomes to mitochondria. *Biochem Biophys Res Commun* **213**, 1035-1041
48. Verhoeven, N. M., Jakobs, C., ten Brink, H. J., Wanders, R. J., and Roe, C. R. (1998) Studies on the oxidation of phytanic acid and pristanic acid in human fibroblasts by acylcarnitine analysis. *Journal of inherited metabolic disease* **21**, 753-760
49. Furihata, T., Hosokawa, M., Nakata, F., Satoh, T., and Chiba, K. (2003) Purification, molecular cloning, and functional expression of inducible liver acylcarnitine hydrolase in C57BL/6 mouse, belonging to the carboxylesterase multigene family. *Arch Biochem Biophys* **416**, 101-109
50. Satoh, T., and Hosokawa, M. (2006) Structure, function and regulation of carboxylesterases. *Chem Biol Interact* **162**, 195-211
51. Antonenkov, V. D., and Hiltunen, J. K. (2012) Transfer of metabolites across the peroxisomal membrane. *Biochim Biophys Acta* **1822**, 1374-1386

Figure Legends

Figure 1. Peroxisomal fatty acid beta-oxidation of lauric acid in HEK-293 cells. (A) Schematic representation of the microsomal, peroxisomal and mitochondrial fatty acid metabolism. 1) Microsomal omega-oxidation converts long-chain fatty acids into long-chain dicarboxylic acids (DCAs), which are subsequently directed to the peroxisome. 2) Long-chain DCA- and acyl-CoAs (and possibly acylcarnitines as demonstrated in this manuscript) enter the peroxisome for further oxidation. Peroxisomal FAO consists of four steps catalyzed by different enzymes and leading to the formation of a chain-shortened acyl-CoA and acetyl-CoA that leave the peroxisome unesterified or as an acylcarnitine. 3) Fatty acids enter mitochondria though the carnitine shuttle, which is composed by carnitine palmitoyltransferase 1 (CPT1), CPT2 and the mitochondrial transporter carnitine acylcarnitine translocase (CACT, SLC25A20). Fatty acids are activated to the respective acyl-CoA ester in the cytosol and converted to acylcarnitines by the action of CPT1, a transmembrane protein of the outer mitochondrial membrane (OMM). These acylcarnitines are then transported across the inner mitochondrial membrane (IMM) by CACT, and once in the matrix reconverted back to acyl-CoAs that will undergo mitochondrial FAO. This cycle can reverse its action in order to export intramitochondrially accumulating acyl-CoAs as acylcarnitine esters. L-aminocarnitine inhibits CPT2 and etomoxir inhibits CPT1. (B) Production of C10-carnitine in the extracellular medium of KO cell lines after loading with C12:0 in the presence of increasing concentrations of the CPT2 inhibitor L-AC. Data are means +/- SEM of duplicates of 2 independent experiments. All experiments were carried out with 2 clonal cell lines. In a regular two-way ANOVA with Tukey's multiple comparisons test, both genotype and L-AC concentration were shown to have a significant effect. The multiple comparisons test yielded significant results at all used L-AC concentrations (except for 0µM). All KO clones except for the *EHHADH* KO differed significantly from WT HEK-293 cells.

Figure 2. ABCD3 is essential for peroxisomal FAO of lauric acid. (A) Production of C10-carnitine in the extracellular medium of *CPT2*, *CPT2*/*PEX13* and *CPT2*/*ABCD3* KO cell lines after incubation with C12:0. Statistical significance was tested using an ordinary one-way ANOVA with Dunnett's multiple comparisons test. **** indicates $P < 0.0001$. (B) Production of C10-carnitine in the extracellular medium of *CPT2* and *CPT2*/*ABCD3* KO cell lines transfected for 24h with an empty plasmid or a plasmid containing the human transporter *ABCD3* (pABCD3) after incubation with C12:0. Statistical significance was tested using an ordinary two-way ANOVA with Bonferroni's multiple comparisons test. * indicates $P < 0.05$. Data are means +/- SEM of duplicates of 2 independent experiments. All experiments were carried out with 2 clonal cell lines.

Figure 3. Peroxisomal FAO of palmitic acid in HEK-293 cells. (A) Production of C10- and C12-carnitine in the extracellular medium of *CPT2*, *CPT2*/*PEX13* and *CPT2*/*ABCD3* KO cell lines after incubation with

palmitate (C16:0). Statistical significance was tested using an ordinary two-way ANOVA with Bonferroni's multiple comparisons test. ** indicates P < 0.01. Data are means +/- SEM of duplicates of 2 independent experiments. All experiments were carried out with 2 clonal cell lines. (B) Production of CO_2 and acid soluble products (ASP) from [1-^{14}C] C16:0 in *CPT2*, *CPT2*/*PEX13* and *CPT2*/*ABCD3* KO cell lines. Statistical significance was tested using an ordinary one-way ANOVA with Dunnett's multiple comparisons test. ** indicates P < 0.01. Data are means +/- SD. We used 3 control, 1 *CPT2*, 1 *CPT2*/*PEX13* and 2 *CPT2*/*ABCD3* independently generated KO cell lines. Each cell line was analyzed in triplicate.

Figure 4. Peroxisomes can accept acylcarnitines as substrate. (A) Production of C10-carnitine after incubation of *CPT2*, *CPT2*/*PEX13* and *CPT2*/*ABCD3* KO cells with lauroylcarnitine (C12-carnitine) and palmitoylcarnitine (C16-carnitine). (B) Production of C10-carnitine after incubation of *CPT2* and *CPT2*/*PEX13* KO cells with C12:0 and C12-carnitine, with and without etomoxir inhibition. (C) Production of C16-carnitine after incubation of *CPT2* and *CPT2*/*CPT1A* KO cell lines with C16:0. (D) Production of C10-carnitine after incubation of *CPT2* and *CPT2*/*CPT1A* KO cell lines with C12:0 or C12-carnitine. (E) Production of C10-carnitine after incubation of *CPT2* and *CPT2*/*CPT1A* KO cell lines with C16:0 or C16-carnitine. Statistical significance was tested using an ordinary two-way ANOVA with Bonferroni's multiple comparisons test. ** indicates P < 0.01. Data are means +/- SEM of duplicates of 2 independent experiments. All experiments were carried out with 2 clonal cell lines. (F) Production of CO_2 and acid soluble products (ASP) from [1-^{14}C] C16-carnitine in *CPT1A*, *CPT2*, *CPT2*/*CPT1A*, *CPT2*/*PEX13* and *CPT2*/*ABCD3* KO cell lines. Statistical significance was tested using an ordinary one-way ANOVA with Dunnett's multiple comparisons test. ** indicates P < 0.01. Data are means +/- SD. We used 3 control, 2 *CPT1A*, 1 *CPT2*, 2 *CPT2*/*CPT1A*, 1 *CPT2*/*PEX13* and 2 *CPT2*/*ABCD3* independently generated KO cell lines. Each cell line was analyzed in triplicate. The inset shows the individual data points for the indicated cell lines.

Figure 5. Peroxisomal acylcarnitines in plasma of WT, *Ehhadh* KO and *Hsd17b4* KO mice treated with L-AC. (A) Concentrations of the C16-, C18:1- and C18-carnitines and the ratio (C16+C18:1)/C2. (B) Concentrations of the C10-, C12- and C14-carnitines. (C) Proportion of cis-5-tetradecenoylcarnitine and myristoleoylcarnitine (cis-9) of the C14:1-carnitine. Plasma acylcarnitine concentrations were measured in overnight fasted WT and *Ehhadh* KO mice treated with saline (n = 7 WT and 5 KO), L-AC (n = 6 WT and 6 KO) or etomoxir (n = 6 WT and 6 KO). Data are means +/- SD. A two-way analysis of variance was performed and the results are displayed in a table for each graph. T, treatment effect; G genotype effect; I interaction term; ns, not significant. (D) Concentrations of the C16:1-, C16-, C18:2-, C18:1- and C18-carnitines and the ratio (C16+C18:1)/C2. (E) Concentrations of the C10-, C12- and C14-carnitines. Plasma acylcarnitine concentrations were measured in 8 hour fasted WT and *Hsd17b4* KO mice treated with L-AC

(n = 8 WT and 8 KO). Data are means +/- SD. The P value was determined using a Mann Whitney test. ** indicates $P < 0.01$ and * indicates $P < 0.05$.

Figure 1

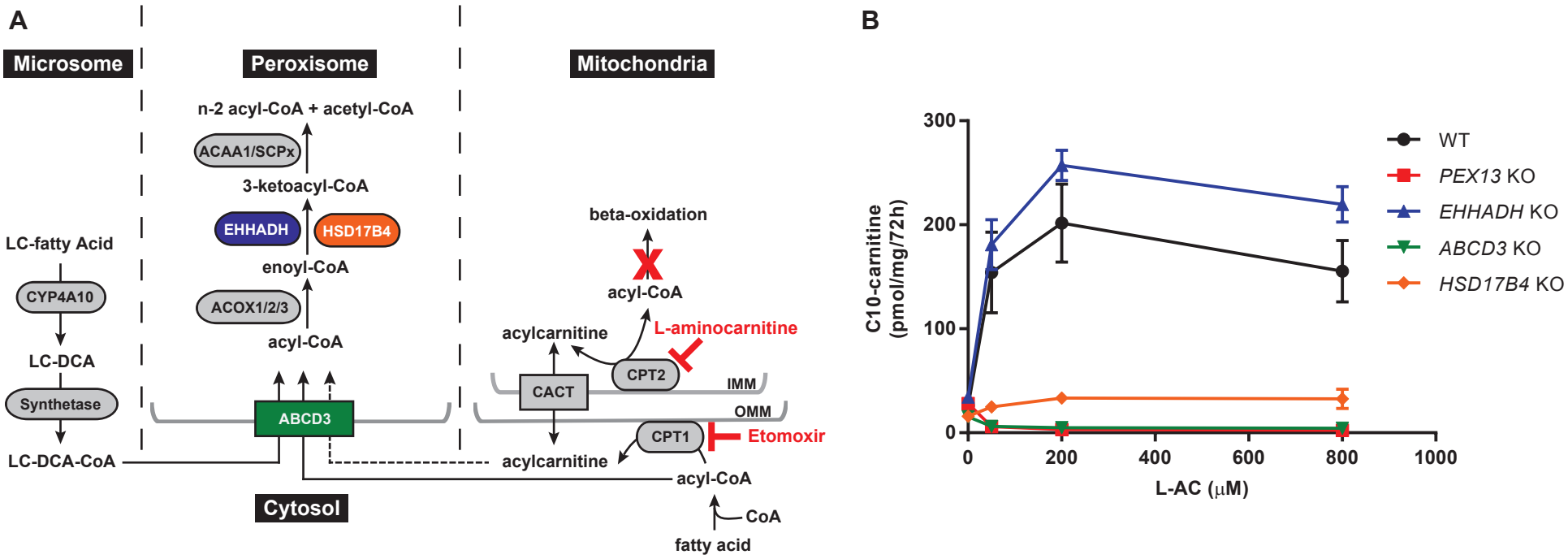
A
Microsome
Peroxisome
Mitochondria
n-2 acyl-CoA + acetyl-CoA
ACAA1/SCPx
3-ketoacyl-CoA
EHHADH
HSD17B4
enoyl-CoA
ACOX1/2/3
acyl-CoA
LC-fatty Acid
CYP4A10
LC-DCA
Synthetase
LC-DCA-CoA
ABCD3
Cytosol
beta-oxidation
acyl-CoA
acylcarnitine
L-aminocarnitine
CPT2
CACT
IMM
OMM
CPT1
Etomoxir
acylcarnitine
acyl-CoA
CoA
fatty acid
B
C10-carnitine (pmol/mg/72h)
300
200
100
0
0
200
400
600
800
1000
L-AC (μM)
WT
PEX13 KO
EHHADH KO
ABCD3 KO
HSD17B4 KO

Figure 2

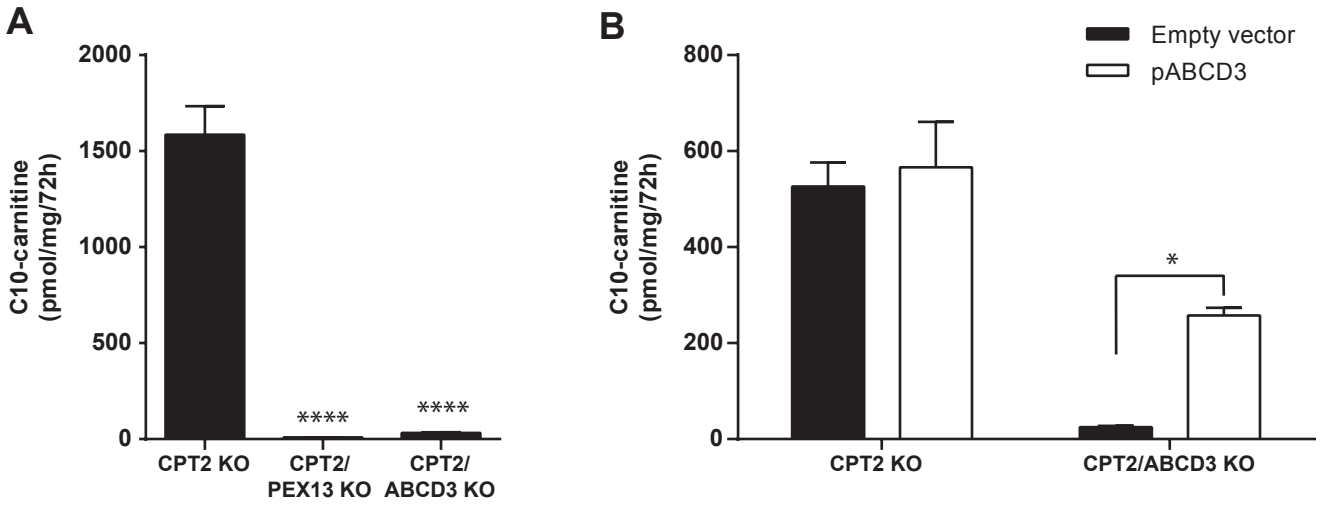
A
2000
1500
1000
500
0
C10-carnitine (pmol/mg/72h)
****
****
CPT2 KO
CPT2/ PEX13 KO
CPT2/ ABCD3 KO
B
800
600
400
200
0
C10-carnitine (pmol/mg/72h)
Empty vector
pABCD3
*
CPT2 KO
CPT2/ABCD3 KO

Figure 3

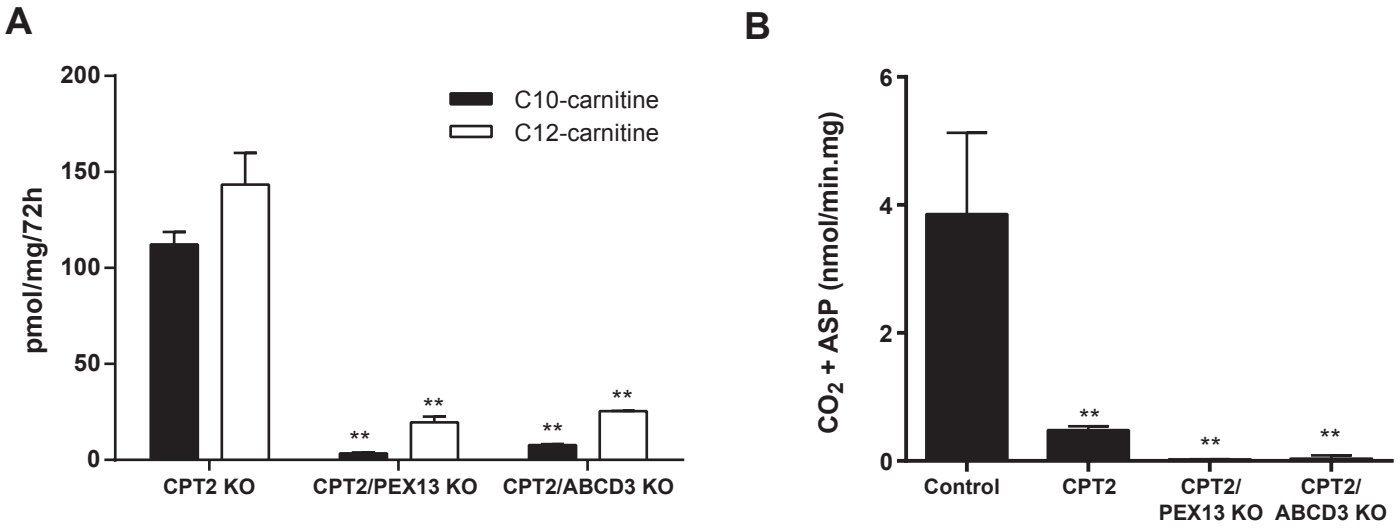
A
200
150
100
50
0
pmol/mg/72h
C10-carnitine
C12-carnitine
**
**
**
**
CPT2 KO
CPT2/PEX13 KO
CPT2/ABCD3 KO
B
6
4
2
0
CO2 + ASP (nmol/min.mg)
**
**
**
Control
CPT2
CPT2/
PEX13 KO
CPT2/
ABCD3 KO

Figure 4

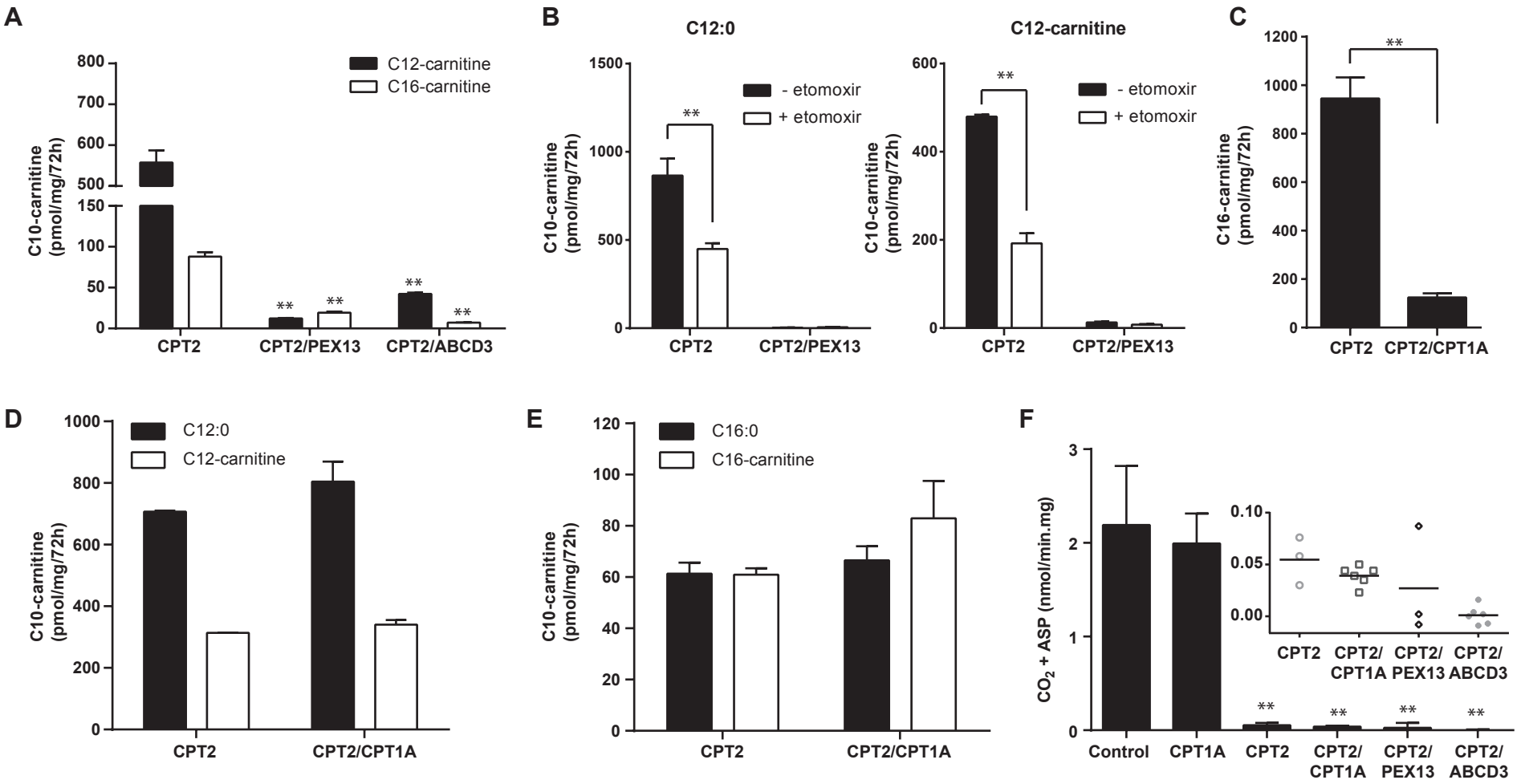
A
C12-carnitine
C16-carnitine
C10-carnitine (pmol/mg/72h)
CPT2
CPT2/PEX13
CPT2/ABCD3
B
C12:0
C12-carnitine
- etomoxir
+ etomoxir
C10-carnitine (pmol/mg/72h)
CPT2
CPT2/PEX13
C
C16-carnitine (pmol/mg/72h)
CPT2
CPT2/CPT1A
D
C12:0
C12-carnitine
C10-carnitine (pmol/mg/72h)
CPT2
CPT2/CPT1A
E
C16:0
C16-carnitine
C10-carnitine (pmol/mg/72h)
CPT2
CPT2/CPT1A
F
CO2 + ASP (nmol/min.mg)
Control
CPT1A
CPT2
CPT2/ CPT1A
CPT2/ PEX13
CPT2/ ABCD3

Figure 5

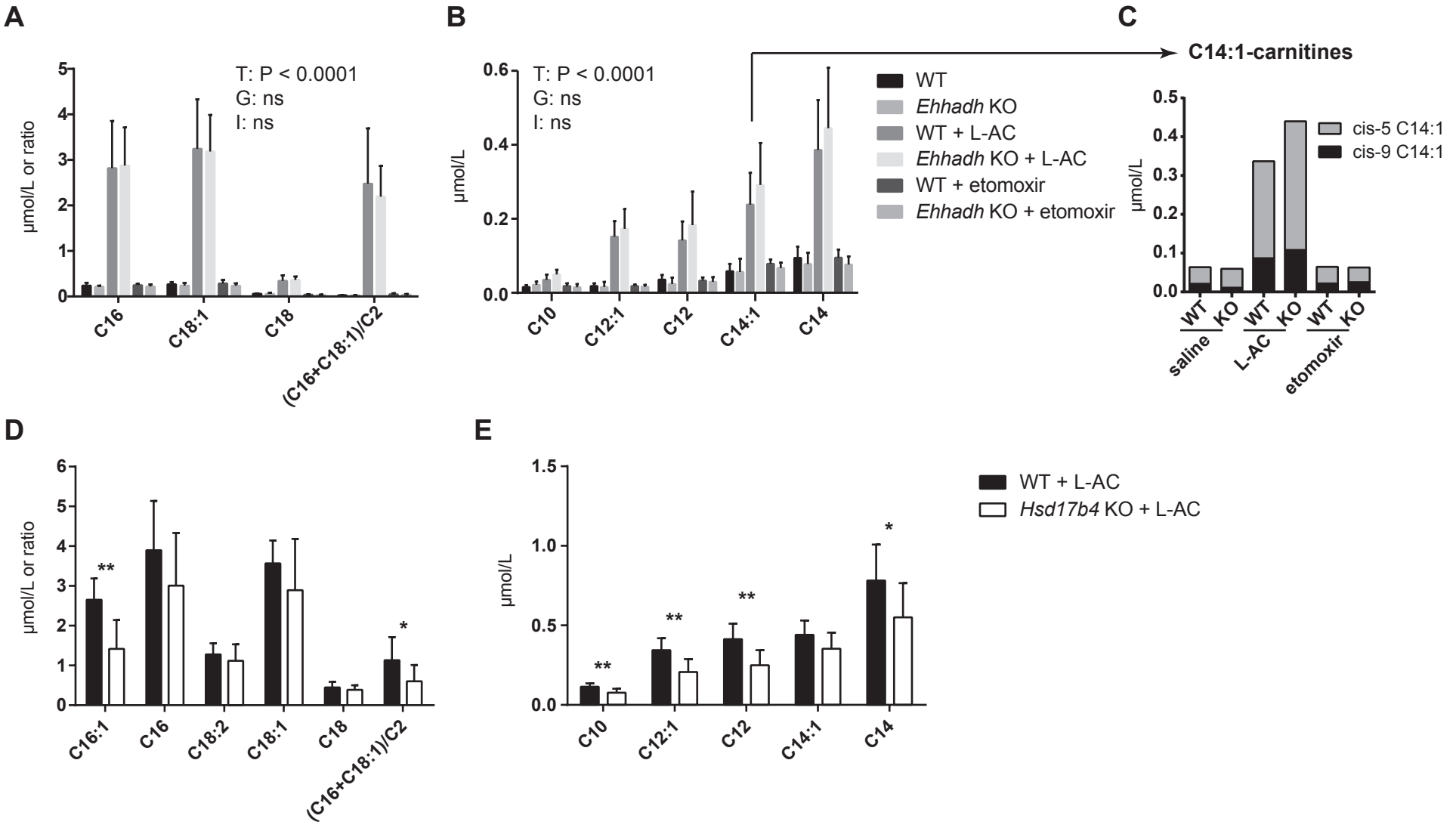
A
T: P < 0.0001
G: ns
I: ns
µmol/L or ratio
C16
C18:1
C18
(C16+C18:1)/C2
B
T: P < 0.0001
G: ns
I: ns
µmol/L
C10
C12:1
C12
C14:1
C14
WT
Ehhadh KO
WT + L-AC
Ehhadh KO + L-AC
WT + etomoxir
Ehhadh KO + etomoxir
C
C14:1-carnitines
µmol/L
cis-5 C14:1
cis-9 C14:1
WT
KO
saline
L-AC
etomoxir
D
µmol/L or ratio
C16:1
C16
C18:2
C18:1
C18
(C16+C18:1)/C2
E
µmol/L
C10
C12:1
C12
C14:1
C14
WT + L-AC
Hsd17b4 KO + L-AC

A

Gene	Expression (TPM)
ABCD1	1.9
ABCD2	0
ABCD3	35.3
HSD17B4	71.8
EHHADH	4.8
CPT2	10.2
CPT1A	5.8
PEX13	8.9

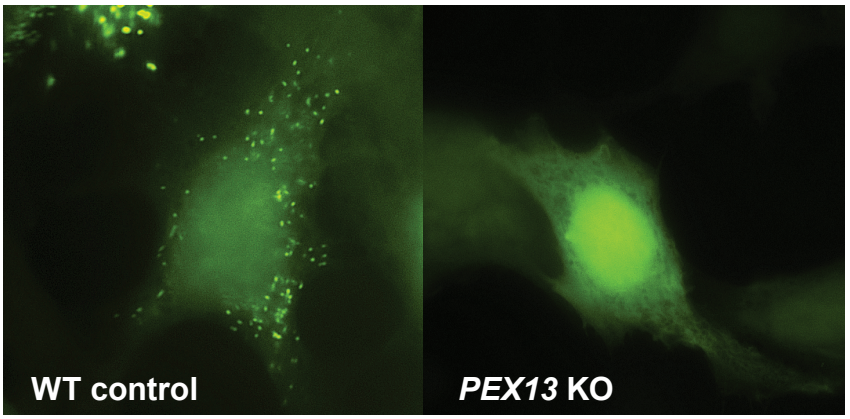

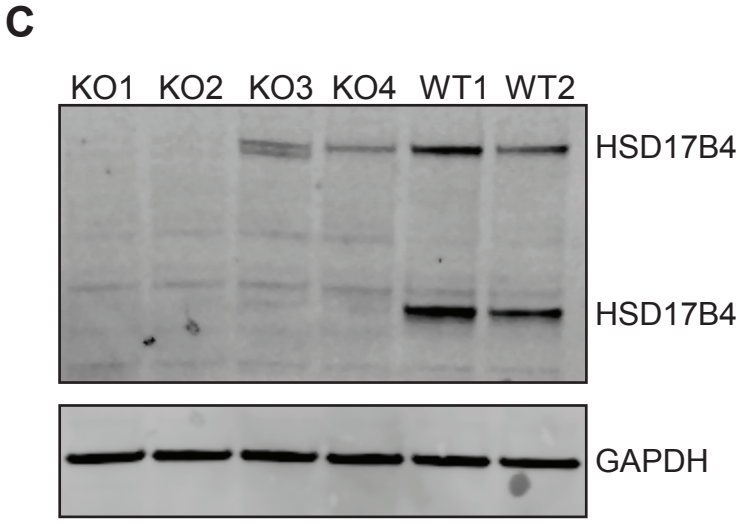

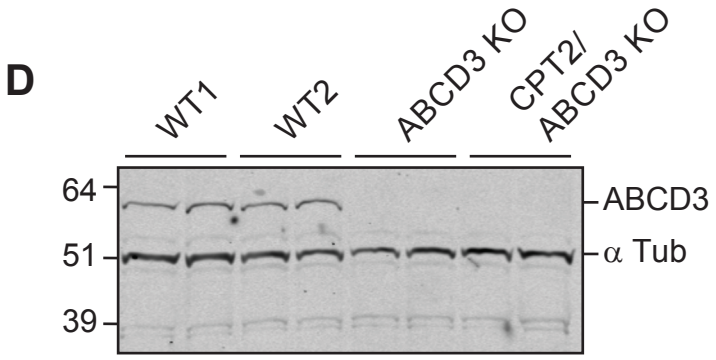

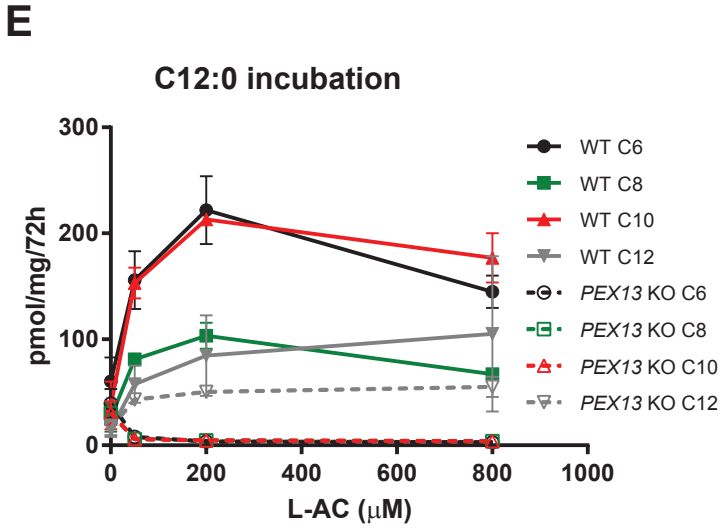

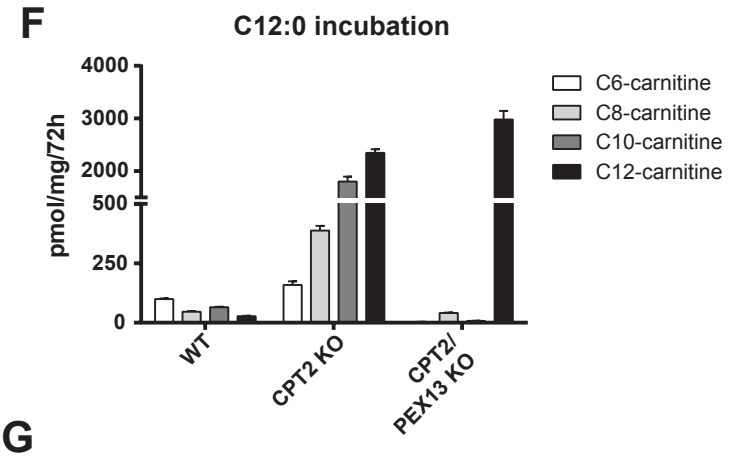

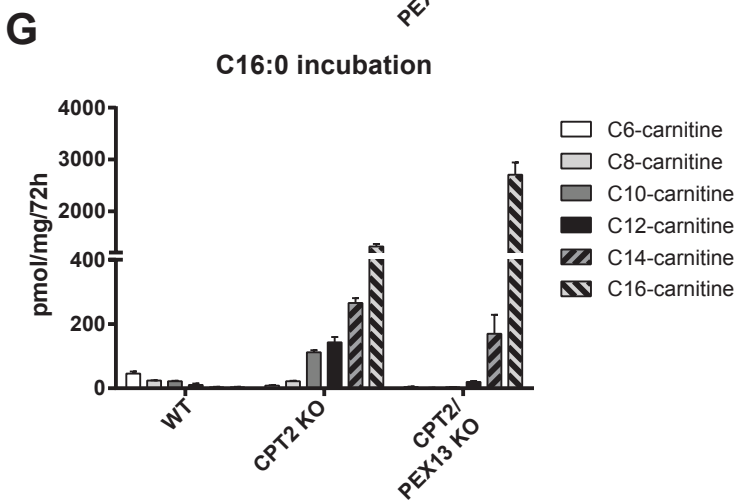

Figure S1. (A) The cell lines of the Human Protein Atlas have been analyzed by RNAseq to estimate the transcript abundance of each protein-encoding gene. We have reproduced the abundance as transcript per million (TPM) for all genes highlighted in this study. (B) Fluorescence microscopy of GFP-SKL in control and *PEX13* KO HEK-293 cells. (C) HSD17B4 immunoblot of 4 KO clones and 2 control HEK-293 samples. The HSD17B4 antibody recognizes the full length (79kD) and a proteolytically processed fragment (45kD; enoyl-CoA hydratase component). KO clones with fully deficient HSD17B4 (KO1 and KO2) were used for our studies. (D) ABCD3 immunoblot of one ABCD3 KO clone, one CPT2/ABCD3 double KO clone and 2 control clones. Each sample was analyzed in duplicate. The position of the molecular weight markers is indicated in kDa. Alpha Tubulin (α Tub) was used as a loading control. (E) Production of C6-, C8-, C10-and C12-carnitine in the extracellular medium of WT and *PEX13* KO clonal cell lines after loading with C12:0 in the presence of increasing concentrations of the CPT2 inhibitor L-AC. Data are means +/- SD of 2 or 4 independent observations. (F) Production of C6-, C8-, C10- and C12-carnitine in the extracellular medium of WT, *CPT2* KO and *CPT2*/*PEX13* double KO clonal cell lines after loading with C12:0. (G) Production of C6-, C8-, C10-, C12-, C14- and C16-carnitine in the extracellular medium of WT, *CPT2* KO and *CPT2*/*PEX13* double KO clonal cell lines after loading with C16:0.

Supplemental Table 1. List of CRISPR-Cas9 KO cell lines generated with their respective mutations.

		Mutations	
Cell line	**Gene(s)**	**Mutation 1**	**Mutation 2**
PEX13 KO	*PEX13*	c.142_146delCTTAC; p.L48Qfs*17	Insertions*
EHHADH KO	*EHHADH*	c.357_358insT; p.V120Cfs*31	c. 357_358insA; p.V120S fs*31
EHHADH KO	*EHHADH*	c.301_302delAC; p.L76Tfs*5	c.301_302delAC; p.L 76 T fs*5
ABCD3 KO	*ABCD3*	c.267_278delTGCTGTTATGCT	c.275_276insT; p.M92Ifs*9
HSD17B4 KO	*HSD17B4*	c.76_76delG; p.A26Pfs*10	c.77_78delCC; p.L27Gfs*13
HSD17B4 KO	*HSD17B4*	c.76_76delG; p.A26Pfs*10	c.76_76delG; p.A26Pfs*10
CPT2 KO	*CPT2*	c.215_216insT; p.L72Ffs*3	c.210_226delTCTCTTGAATGATGGCC; p.L71Vfs*12
CPT1A KO	*CPT1A*	c.40_60delinsTTCA; p.V14Ffs*7	c.40_60delinsTTCA; p.V14Ffs*7
CPT1A KO	*CPT1A*	c.61_71delCTGCGGCTGAG; L21Pfs*2	insertion of ~50bp
CPT2/PEX13 KO	*CPT2*	c.215_216insT; p.L72Ffs*3	c.215_216insT; p.L72Ffs*3
	PEX13	c.142_146delCTTAC; p.L48Qfs*17	Insertions*
CPT2/PEX13 KO	*CPT2*	c.299_301delTTG	c.299_302delTTGC; p.A101Wfs*28
	PEX13	c.142_146delCTTAC; p.L48Qfs*17	Insertions*
CPT2/ABCD3 KO	*CPT2*	c.213_214insT; p.L72Ffs*3	c.213_214insT; p.L72Ffs*3
	ABCD3	c.267_278delTGCTGTTATGCT	c.275_276insT; p.M92Ifs*9
CPT2/ABCD3 KO	*CPT2*	c.213_214insT; p.L72Ffs*3	c.215_215delT; p.L72*
	ABCD3	c.267_278delTGCTGTTATGCT	c.275_276insT; p.M92Ifs*9
CPT2/CPT1A KO	*CPT2*	c.215_216insT; p.L72Ffs*3	c.210_226delTCTCTTGAATGATGGCC; p.L71Vfs*12
	CPT1A	c.41_53delTCACTCCGGACGG; p.V14Gfs*6	insertion of ~147bp
CPT2/CPT1A KO	*CPT2*	c.215_216insT; p.L72Ffs*3	c.210_226delTCTCTTGAATGATGGCC; p.L71Vfs*12
	CPT1A	c.40_74delinsC; p.V14Lfs*45	c.40_74delinsC; p.V14Lfs*45

*We selected clones with apparent homozygous or compound heterozygous mutations. Given that HEK-293 cells are near triploid this means that for cells that appeared compound heterozygous, one of the two mutations is likely biallelic. For *PEX13* we did not obtain such clones. In addition to one allele with a 5bp deletion, these clones contained two other alleles containing insertions (~60 and ~80 basepairs).